

Modular Assembly and Air-Stable Electrochemistry of Ruthenium Porphyrin Monolayers

Todd A. Eberspacher,[†] James P. Collman,^{*,†} Christopher E. D. Chidsey,^{*,†}
Deirdre L. Donohue,[‡] and Hal Van Ryswyk^{*,‡}

Department of Chemistry, Stanford University, Stanford, California 93405,
and Department of Chemistry, Harvey Mudd College, Claremont, California 91711

Received December 3, 2002. In Final Form: February 24, 2003

Two approaches are presented to the modular construction of alkanethiolate self-assembled monolayers (SAMs) on gold surfaces selectively decorated with metalloporphyrins. In the first approach, an isonicotinate ligand is incorporated into the SAM via deposition from a two-component solution. In the second approach, a pyridine or imidazole ligand is attached to the SAM after self-assembly via carbodiimide-induced amide linkages to terminal carboxylates. Subsequent derivatization of monolayers formed in either of these ways with metalloporphyrins of the type Ru(POR)(CH₃CN)₂, where POR = octaethylporphyrin or meso-tetratoluyloporphyrin, creates apically bound metalloporphyrins that exhibit sharp, stable cyclic voltammetric features in methylene chloride or water under ambient atmosphere. The presence of hexafluorophosphate in the supporting electrolyte is critical in evincing near-ideal electrochemistry. While the identity of the distal axial ligand under ambient atmosphere is unknown, this ligand can be readily and irreversibly exchanged with pyridine or other heterocyclic nitrogen donors. These approaches can be used to create previously unavailable asymmetrically substituted metalloporphyrins which can function as templates for additional modular modification of the monolayer/solution interface.

Introduction

A wide range of electroactive, fluorescent, or chromophoric molecules have been tethered to metal surfaces via alkanethiolate appendages. At first glance, such an approach offers an attractive method for immobilizing interesting molecules on a surface: inclusion of an alkanethiol side chain usually ensures chemisorption of a monolayer or submonolayer of material. This approach has successfully immobilized porphyrins and other large, complex supramolecular assemblies onto gold surfaces.^{1–11}

However, as the molecule targeted for surface immobilization becomes larger, more complex, or charged, this simplistic approach to surface decoration often leads to poorly formed monolayers with limited long-range order, or no monolayer formation at all. Some target systems are intolerant of the thiol appendage, while other large target systems cannot form orderly monolayers because the pendant molecule will not pack efficiently.¹³ The

incorporation of charged centers presents additional challenges, often based upon the mismatch of intermolecular forces present.¹⁴ In certain charged systems, well-formed monolayers do not self-assemble, even with substantial amounts of unsubstituted diluent thiols present.¹⁵ Finally, even when charge, cross-sectional area, and intermolecular forces do not impede monolayer formation, the inclusion of an alkanethiol appendage may prove synthetically challenging.

Recent reports have demonstrated the modular assembly of complex molecules on preformed self-assembled monolayers (SAMs). In this approach, a well-formed monolayer is tagged with a ligand or reactive center for subsequent ligand attachment. The target molecule is subsequently attached to the monolayer-bound ligand expressed on the surface, typically making use of gentle reaction conditions which will not perturb the underlying monolayer structure. In this fashion, the underlying monolayer, the point of attachment, and the coupling chemistry can be considered individually and sequentially. Examples of this approach include the attachment of metalloporphyrins,^{16–21} metallophthalocyanines,^{22,23} and

* Corresponding authors. E-mail: Hal_VanRyswyk@hmc.edu.

[†] Department of Chemistry, Stanford University.

[‡] Department of Chemistry, Harvey Mudd College.

(1) Imahori, H.; Norieda, H.; Ozawa, S.; Ushida, K.; Yamada, H.; Azuma, T.; Tamaki, K.; Sakata, Y. *Langmuir* **1998**, *14*, 5335–5338.

(2) Imahori, H.; Ozawa, S.; Ushida, K.; Takahashi, M.; Azuma, T.; Ajavakom, A.; Akiyama, T.; Hasegawa, M.; Taniguchi, S.; Okada, T.; Sakata, Y. *Bull. Chem. Soc. Jpn.* **1999**, *72*, 485–502.

(3) Imahori, H.; Yamada, H.; Ozawa, S.; Ushida, K.; Sakata, Y. *Chem. Commun.* **1999**, 1165–1166.

(4) Imahori, H.; Hasobe, T.; Yamada, H.; Nishimura, Y.; Yamazaki, I.; Fukuzumi, S. *Langmuir* **2001**, *17*, 4925–4931.

(5) Kondo, T.; Ito, T.; Nomura, S.-i.; Uosaki, K. *Thin Solid Films* **1996**, *284–285*, 652–655.

(6) Uosaki, K.; Kondo, T.; Zhang, X.-Q.; Yanagida, M. *J. Am. Chem. Soc.* **1997**, *119*, 8367–8368.

(7) Redman, J. E.; Sanders, J. K. M. *Org. Lett.* **2000**, *2*, 4141–4144.

(8) Boeckl, M. S.; Bramblett, A. L.; Hauch, K. D.; Sasaki, T.; Ratner, B. D.; Rogers, J. W., Jr. *Langmuir* **2000**, *16*, 5644–5653.

(9) Gryko, D. T.; Zhao, F.; Yasserli, A. A.; Roth, K. M.; Bocian, D. F.; Kuhr, W. G.; Lindsey, J. S. *J. Org. Chem.* **2000**, *65*, 7356–7362.

(10) Gryko, D. T.; Clausen, C.; Roth, K. M.; Dontha, N.; Bocian, D. F.; Kuhr, W. G.; Lindsey, J. S. *J. Org. Chem.* **2000**, *65*, 7345–7355.

(11) Yamada, T.; Hashimoto, T.; Kikushima, S.; Ohtsuka, T.; Nango, M. *Langmuir* **2001**, *17*, 4634–4640.

(12) Mrksich, M. *Chem. Soc. Rev.* **2000**, *29*, 267–273.

(13) Ashkenasy, G.; Kalyuzhny, G.; Libman, J.; Rubinstein, I.; Shanzler, A. *Angew. Chem., Int. Ed.* **1999**, *38*, 1257–1261.

(14) Doblhofer, K.; Figura, J.; Fuhrhop, J.-H. *Langmuir* **1992**, *8*, 1811–1816.

(15) Obeng, Y. S.; Bard, A. J. *Langmuir* **1991**, *7*, 195–200.

(16) Offord, D. A.; Sachs, S. B.; Ennis, M. S.; Eberspacher, T. A.; Griffin, J. H.; Chidsey, C. E. D.; Collman, J. P. *J. Am. Chem. Soc.* **1998**, *120*, 4478–4487.

(17) Li, D.; Moore, L. W.; Swanson, B. I. *Langmuir* **1994**, *10*, 1177–1185.

(18) Pilloud, D. L.; Moser, C. C.; Reddy, K. S.; Dutton, P. L. *Langmuir* **1998**, *14*, 4809–4818.

(19) Cruz, F. D.; Driaf, K.; Berthier, C.; Lameille, J.-M.; Armand, F. *Thin Solid Films* **1999**, *349*, 155–161.

(20) Zhang, Z.; Imae, T.; Sato, H.; Watanabe, A.; Ozaki, Y. *Langmuir* **2001**, *17*, 4564–4568.

(21) Zou, S.; Clegg, R. S.; Anson, F. C. *Langmuir* **2002**, *18*, 3241–3246.

(22) Huc, V.; Bourgoin, J.-P.; Bureau, C.; Valin, F.; Zalczer, G.; Palacin, S. *J. Phys. Chem. B* **1999**, *103*, 10489–10495.

tetraammineruthenium complexes²⁴ to monolayer-tethered ligands and the use of gentle conditions to anchor the ligand of a prebuilt transition metal complex to a monolayer-bound reactive center.^{24,25}

The advantages of modular assembly are severalfold: The individual components of the overall structure can be synthesized and characterized separately. Ligands that may impede or prevent compact monolayer assembly can be introduced afterward; complicated structures that may not self-assemble in their final form can be built and characterized stepwise. Given the inherent control in modular assembly, this method allows finer control of surface site concentrations. Once a library of components (monolayers, ligands, and targets) has been synthesized, a wide array of related structures can be assembled quickly. Borrowing an analogy from the Merrifield synthesis of polypeptides,²⁶ increasingly complex structures can be built and purified on the templates created via modular assembly.

A number of traditional multilayer approaches fall within the modular assembly framework. Langmuir–Blodgett films,²⁷ metal phosphonate^{28–30} and sulfonate³¹ multilayers, and polyelectrolyte multilayers^{32–34} are all constructed in a stepwise, layer-by-layer fashion. However, each of these approaches requires a charged species at the monolayer/solution interface during construction. The approach we favor, axial ligation of transition metal complexes, does not suffer from this fundamental limitation. By selection of appropriate neutral ligands and metal complexes with sufficient kinetic and thermodynamic stability, enhanced lateral spatial control is achieved during monolayer construction. The ability to readily control the number of reactive sites expressed on the outer edge of a monolayer assembly offers an additional degree of regulation in constructing customized surfaces and templates for further construction. We seek to generalize the axial ligation approach across a number of pendant ligands and transition metal complexes.

We report here the modular formation of monolayer assemblies containing axially ligated metalloporphyrins, offering two different synthetic routes to such structures. The electrochemistry of such structures is presented, showing that modular construction leads to greater control over the electrochemical properties of such supramolecular structures. Additional insights are presented regarding the stability of axially ligated metalloporphyrin structures under ambient atmosphere, the conditions required to observe ideal electrochemical response in such systems, and the possibility of using these systems as templates for extended supramolecular construction.

(23) Huc, V.; Saveyroux, M.; Bourgoïn, J.-P.; Valin, F.; Zalczer, G.; Albouy, P.-A.; Palacin, S. *Langmuir* **2000**, *16*, 1770–1776.

(24) Luo, J.; Isied, S. S. *Langmuir* **1998**, *14*, 3602–3606.

(25) Brevnov, D. A.; Finklea, H. O.; Van Ryswyk, H. *J. Electroanal. Chem.* **2001**, *500*, 100–107.

(26) Birr, C. *Aspects of the Merrifield Peptide Synthesis*; Springer: New York, 1978.

(27) Ulman, A. *An Introduction to Ultrathin Organic Films From Langmuir–Blodgett to Self-Assembly*; Academic Press: San Diego, 1991.

(28) Lee, H.; Kepley, L. J.; Hong, H.-G.; Mallouk, T. E. *J. Am. Chem. Soc.* **1988**, *110*, 618–620.

(29) Putvinski, T. M.; Schilling, M. L.; Katz, H. E.; Chidsey, C. E. D.; Muijsce, A. M.; Emerson, A. B. *Langmuir* **1990**, *6*, 1567–1571.

(30) Katz, H. E. *Chem. Mater.* **1994**, *6*, 2227–2232.

(31) Bakiamoh, S. B.; Blanchard, G. J. *Langmuir* **1999**, *15*, 6379–6385.

(32) Fendler, J. H. *Chem. Mater.* **1996**, *8*, 1616–1624.

(33) Mallouk, T. E.; Kim, H.-N.; Ollivier, P. J.; Keller, S. W. *Ultrathin Films Based on Layered Materials*; Alberti and Giulio; Bein, T., Ed.; Elsevier: Oxford, U.K., 1996; Vol. 7, pp 189–217.

(34) Decher, G. *Layered Nanoarchitectures via Directed Assembly of Anionic and Cationic Molecules*; Sauvage, J.-P., Hosseini, M. W., Eds.; Elsevier: Oxford, U.K., 1996; Vol. 9, pp 507–528.

Experimental Section

General. Manipulations of oxygen- and water-sensitive compounds were performed in a nitrogen-filled Vacuum Atmospheres Co. drybox maintained at or below 2 ppm O₂. Oxygen levels were monitored with an AO 316-C trace oxygen analyzer.

Reagents. Toluene was distilled from sodium and benzophenone and then subjected to three freeze/pump/thaw cycles before use. Methylene chloride was distilled from calcium hydride. Tetrabutylammonium hexafluorophosphate (TBAH) (Aldrich) was recrystallized three times from ethanol. Decanethiol, nonanethiol, 11-mercaptoundecanoic acid (MUA), pyridine, pyrazine, and 4,4'-dipyridyl (Aldrich), 1-ethyl-3-(3-dimethylaminopropyl)carbodiimide (EDC) (Sigma), and ethanol (Pharmco) were used as received.

Bis-acetonitrile octaethylporphyrinatoruthenium(II), bis-acetonitrile *meso*-tetratoluyloporphyrinatoruthenium(II),¹⁶ 11-mercaptoundecylisonicotinate³⁵ (MUIN), 10-mercaptodecan-1-ol, 9-mercaptanonan-1-ol,³⁶ and isopropyl isonicotinate³⁷ were prepared via literature procedures.

In a typical preparation for amides of MUA, 321 mg (3 mmol) of 4-(aminomethyl)pyridine, 654 mg (3 mmol) of MUA, 618 mg (3 mmol) of dicyclohexylcarbodiimide, and 405 mg (3 mmol) of 1-hydroxybenzotriazole were refluxed in 20 mL of tetrahydrofuran (THF) under nitrogen for 10 h. After cooling to room temperature, the dicyclohexylurea was filtered off, and the filtrate was combined with 40 mL of ethyl acetate. The organic layer was extracted three times with 20 mL of 10% citric acid solution and three times with 20 mL of saturated sodium bicarbonate solution and then dried over sodium sulfate prior to isolation of the product via rotary evaporation. Typical yields were 80%. 400 MHz ¹H NMR (CDCl₃, δ): 8.56 (d, 2H, *J* = 6 Hz, py), 7.21 (d, 2H, *J* = 6 Hz, py), 5.91 (t, 1H, *J* = 6 Hz, NH), 4.47 (d, 2H, *J* = 6 Hz, pyCH₂N), 2.53 (q, 2H, *J* = 7 Hz, CH₂S), 2.27 (t, 2H, *J* = 8 Hz, CH₂CO), 1.64 (m, 4H, methylene), 1.32 (m, 12H, methylene). IR (CDCl₃, cm⁻¹): 3450 (N–H str), 2930 (CH₂ as), 2856 (CH₂ sym), 1672 (C=O str), 1512 (N–H ipb).

Substrates. Titanium and gold were evaporated sequentially on cleaned silicon wafers in a manner described previously.¹⁶

Monolayer Formation. Two-component deposition solutions of varying mole fractions were prepared in absolute ethanol with a total thiol concentration of 1.25 mM. Gold substrates were cleaned by immersion in “piranha” solution (3:1 v/v H₂SO₄/30% aqueous H₂O₂) for 10 s, followed by rinsing with deionized water and ethanol. (*Warning.* Piranha solution reacts violently, even explosively, with organic materials.^{38–40} It should not be stored or combined with significant quantities of organic material.) The cleaned substrates were immersed in the deposition solutions for 12 h, after which they were rinsed with anhydrous ethanol and blown dry with nitrogen.

Monolayer Derivatization. In a typical conversion, a mixed monolayer containing MUA diluted in nonanethiol was placed in a 25 mM solution of either 4-(aminomethyl)pyridine or 1-(3-aminopropyl)imidazole and 25 mM EDC buffered to pH 8.9 with sodium borate/hydrochloric acid (0.1 M buffer capacity) for 10–90 min. Following conversion, the samples were rinsed with ethanol and blown dry with nitrogen.

Porphyrin Deposition. In an inert atmosphere box, metalloporphyrins were deposited onto SAMs from 0.1 mM solutions in toluene for 2 h. The gold surfaces were rinsed with toluene inside the box and allowed to dry. After removal from the box, samples were rinsed again with toluene and methylene chloride.

Distal Axial Ligand Exchange. Distal axial ligand exchange was accomplished with 10 mM solutions of the appropriate ligand in toluene for a period of 0.5–10 h.

(35) Van Ryswyk, H.; Turtle, E. D.; Watson-Clark, R.; Tanzer, T. A.; Herman, T. K.; Chong, P. Y.; Waller, P. J.; Taurog, A. L.; Wagner, C. E. *Langmuir* **1996**, *12*, 6143–6150.

(36) Bain, C. D.; Troughton, E. B.; Tao, Y.-T.; Evall, J.; Whitesides, G. M.; Nuzzo, R. G. *J. Am. Chem. Soc.* **1989**, *111*, 321–335.

(37) Van Ryswyk, H.; Hinds, B. R. I.; Simmons, B. L.; Solomon, D. S. *J. Electrochem. Soc.* **1992**, *139*, 3098–3102.

(38) Dobbs, D. A.; Bergman, R. G.; Theopold, K. H. *Chem. Eng. News* **1990**, *26*, 2.

(39) Matlow, S. L. *Chem. Eng. News* **1990**, *30*, 2.

(40) Wnuk, T. *Chem. Eng. News* **1990**, *26*, 2.

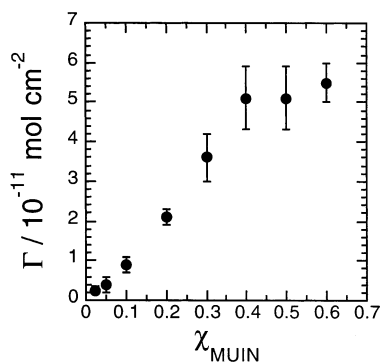


Figure 2. Surface coverage of Ru(TTP) on MUIN monolayers prepared by deposition from a two-component solution of MUIN and decanethiol in ethanol. $C_{\text{thiols}} = 1.25 \text{ mM}$. Metalloporphyrin attachment was accomplished as described in the text. Surface coverages were determined by integration of CV peaks. Error bars reflect the standard deviation of five separate samples.

As shown in the narrow-range scan in Figure 1A, there is an increase in background current following oxidation of the ruthenium center. Cycling to +0.9 V versus SCE (not shown) yields a larger increase in background relative to the narrow-range scan, but still no change in the fwhm of the Ru^{III} reduction wave or its integrated faradaic charge. After a few seconds at 0 V versus SCE or open circuit, the background current returns to the value originally seen in the narrow-range scan. Scanning to still more positive potentials produces permanent changes in the monolayer/metalloporphyrin system: The overall background current increases, the reduction wave associated with the ruthenium center is broadened, and there is loss of electroactive material as measured by the integrated faradaic charge associated with this reduction.

Stability. The electrochemistry of MUIN-based Ru(POR) monolayers is stable for hours in air. Electrodes can be washed repeatedly with toluene or methylene chloride without loss of electroactive material. Electrodes subjected to sonication in methylene chloride for 2–10 min showed minimal loss of electroactive material in the range of 5–15%. Electrodes potentiostated at 0.0 or +0.5 V versus SCE or left at open circuit for 3 h showed the same electroactive surface coverage as freshly prepared electrodes with no degradation of signal. In long-term stability experiments, monolayers of Ru(TTP) on MUIN were left in the drybox under laboratory lighting, on the benchtop under laboratory lighting, and on the benchtop covered with foil. After 72 h, only the samples exposed to both air and light had degraded, retaining less than 2% of their initial electroactive coverage. All other samples showed no degradation.

Surface Coverage. Figure 2 shows the electroactive surface coverage of Ru(TTP) on MUIN/ C_{10} monolayers as a function of deposition solution composition. The limiting surface coverage of $5.7 \times 10^{-11} \text{ mol cm}^{-2}$ found for Ru(TTP) is similar to that obtained for Ru(OEP) in an imidazole-based system.¹⁶ At surface coverages greater than $3.0 \times 10^{-11} \text{ mol cm}^{-2}$, a second, smaller, reversible redox wave is frequently observed at approximately 0.3 V more positive than the $\text{Ru}^{\text{II/III}}$ couple with both Ru(TTP) and Ru(OEP).

Aqueous Electrochemistry. A cyclic voltammogram for Ru(TTP) on a MUIN/ C_{10} monolayer in aqueous 0.5 M perchloric acid supporting electrolyte is shown in Figure 3. The general shape of the ruthenium-based oxidation and reduction is similar to that observed with aqueous lithium chloride supporting electrolyte: a very broad wave with no identifiable peak. Aqueous sodium sulfate, sodium

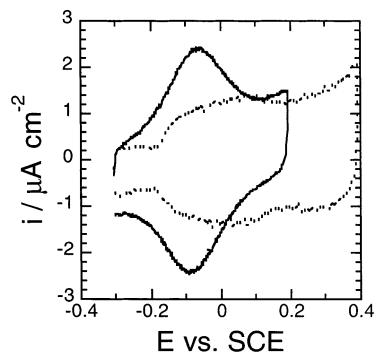


Figure 3. Cyclic voltammograms of Ru(TTP) on MUIN monolayers prepared by deposition from a two-component solution of MUIN and decanethiol in ethanol ($\chi_{\text{MUIN}} = 0.2$, $C_{\text{thiols}} = 1.25 \text{ mM}$). Metalloporphyrin attachment was accomplished as described in the text. (···) Supporting electrolyte of 0.5 M HClO_4 in water; (—) supporting electrolyte of 0.5 M HClO_4 + 0.5 M NH_4PF_6 in water. The scan rate is 0.4 V s^{-1} .

phosphate, and sodium tetrafluoroborate supporting electrolytes as well as acetonitrile with TBAH or tetrabutylammonium perchlorate supporting electrolytes produced less distinct waves which often could not be differentiated from the baseline. In all cases, the electroactive surface coverage, as determined by integration of the current, was lower than that of identical samples which were run in methylene chloride with TBAH.

Addition of 0.5 M ammonium hexafluorophosphate to 0.5 M aqueous perchloric acid yields the second cyclic voltammogram shown in Figure 3. The 150 mV fwhm is slightly larger than that seen in methylene chloride. The electroactive surface coverage is identical to that of samples which were run in methylene chloride.

Samples initially subjected to aqueous electrochemistry could be rinsed thoroughly and then transferred to methylene chloride with TBAH, yielding sharp cyclic voltammograms. This was true in all cases, including those where the aqueous electrochemistry was indistinct. Samples subsequently rinsed and then transferred back into aqueous electrolytes evinced cyclic voltammetry identical to that of freshly prepared samples subjected to these electrolytes.

In an effort to determine if the interaction between the tethered metalloporphyrin and the underlying diluent thiol affects the aqueous electrochemistry, monolayers of constant χ_{MUIN} were assembled using 10-mercaptodecan-1-ol, 9-mercaptanonan-1-ol, or nonanethiol as the diluent thiol. While the electroactive surface coverage increased, as expected for monolayer deposition from ethanol solution in each of these cases relative to that of decanethiol as the diluent thiol, the shape of the ruthenium porphyrin wave in aqueous electrolyte did not differ across any of the diluent thiols used.

Physisorption. In an effort to rule out physisorption of Ru(POR) on the monolayer surface, two separate control experiments were performed. In the first case, monolayers were composed solely of decanethiol, whereas in the second case monolayers were constructed from the amide of benzylamine and MUA, diluted in decanethiol to the same mole fraction as the MUIN monolayers employed in Figure 1. Both of these monolayers were treated with Ru(TTP)- $(\text{CH}_3\text{CN})_2$; in neither case was any electroactive material observed.

Distal Ligand Exchange. Once a ruthenium porphyrin has coordinated to the monolayer, the distal axial ligand can be exchanged in 10 mM solutions of ligand in toluene under dinitrogen or ambient atmosphere over periods ranging from 0.5 to 10 h. Such conditions did not

leach or remove the ruthenium porphyrin from the monolayer surface, nor did the capacitance of the monolayer increase. In cases where the formal potential of the ruthenium porphyrin after exchange differed from that of the precursor complex, exchange could be monitored via cyclic voltammetry so long as care was taken to rinse excess ligand from the electrode prior to performing the scan. Attempts to monitor surface coverages in the presence of pyridine or pyrazine led to stripping of the alkanethiolate from the gold electrode as evidenced by large increases in background capacitance and a subsequent increase in contact angles.

In-Place Conversion. Monolayers of MUA or MUA diluted in nonanethiol were partially converted to the corresponding amides via treatment with an aqueous solution of EDC. While 4-(aminomethyl)pyridine coordinated to pentaammineruthenium(II) has been successfully coupled to MUA monolayers at pH 7,^{24,25} present efforts to attach free 4-(aminomethyl)pyridine at moderate pH were unsuccessful. Use of a borate buffer at pH 8.9 did produce satisfactory coupling. The extent of coupling could be controlled by varying the reaction time over the range of 10–90 min. The use of a diluent thiol produced quicker couplings relative to homogeneous MUA monolayers to achieve a given surface coverage (as determined by electroactivity of Ru(TTP) after treatment), most likely due to greater access of reagents to the monolayer-confined carbonyl carbon. The presence of a diluent thiol also decreased the likelihood that a portion of the MUA monolayer would desorb during the conversion. Monolayers with a large fraction of diluent thiols presumably form more compact, defect-free structures that are less likely to allow access to the thiolate headgroup.

Discussion

Scheme 1 shows two routes to the modular assembly of Ru(POR) systems. The advantages of the first approach include finer, more reproducible control of the number of ligand sites presented for metalloporphyrin attachment. Advantages associated with the second approach include the ability to assemble a range of analogous systems with differing chain lengths or ligands quickly from commercially available components.

With respect to the second approach, the reaction times for the conversion of homogeneous monolayers of ω -mercaptocarboxylic acids to corresponding pyridine-terminated amides increases with carboxylic acid chain length. This is most likely due to an increase in the rigidity of the monolayer with longer chain length. Monolayers comprised of shorter chains ($n < 12$) tend to have a more liquidlike composition,⁴² with a concomitant increase in the mobility of the terminal carboxylates.⁴³ Such increases in monolayer rigidity with increasing chain length mean that reaction times which are sufficient for 10% conversion on a MUA monolayer may lead to very little conversion on a monolayer of 16-mercaptohexadecanoic acid. To circumvent the variation in reaction time required to reach a given degree of derivatization, mixed monolayers of ω -mercaptocarboxylic acids in slightly shorter n -alkanethiols were used. In this fashion, a consistent set of reaction conditions yields similar degrees of derivatization across all chain lengths studied, presumably by allowing nucleophilic substitution at the SAM carbonyl carbon to proceed with less steric hindrance.

Electrochemistry in Methylene Chloride. While methylene chloride is not widely used as a solvent for

electrochemical characterization of alkanethiolate monolayers on gold, detailed studies have shown the gold–thiolate linkage to be stable for extended periods when the potential excursions are limited to a potential range of -0.4 to $+0.5$ V versus SCE.^{44,45} Outside this range, the monolayer half-life quickly decreases to the order of a few minutes. For the work reported here, the ruthenium-based oxidations and reductions are positioned within the zone of extended stability. Repeated cycling through the Ru^{II/III} waves produces little monolayer decomposition.

Clearly there is an increase in monolayer capacitance upon oxidation of the ruthenium center as evidenced by larger baseline currents upon scan reversal at more positive potentials than those observed prior to the wave. There are additional increases in monolayer capacitance that occur at more positive potentials, possibly due to the reversible intercalation of hexafluorophosphate anions within the monolayer. Some of these changes at more positive potentials occur in the absence of a surface-confined electroactive species. Finally, scanning to still more positive potentials required to oxidize the porphyrin ring irreversibly degrades the monolayer structure and may damage the metalloporphyrin, as illustrated by the permanent increase in monolayer capacitance, broadening of the ruthenium reduction wave, and loss of electroactive material.

The second, smaller wave observed approximately 0.3 V positive of the Ru^{II/III} couple at higher surface coverages is likely due to electrostatic effects associated with the additional energy required to oxidize a neutral metalloporphyrin in the midst of the closely packed, uncompensated charge associated with multiple contiguous, oxidized nearest neighbors. These second waves first appear when surface coverages are sufficiently high to have appreciable numbers of porphyrins with three or more contacting nearest neighbors. In a similar fashion, the second waves could also be explained by a fraction of adjacent porphyrins having significant overlap in a sort of “slipped-disk” architecture that would be more common at higher surface coverages. Oxidation of the first metalloporphyrin in a slipped-disk pair would occur at the normal redox potential, while the second would be oxidized at a higher potential due to electrostatic interactions with the overlapped, oxidized metalloporphyrin. We are unable to differentiate between these two related possibilities at present, but ongoing efforts in our laboratories studying axially linked metalloporphyrin oligomers in a “shish-kebab” orientation may provide additional insight.

SAM/Metalloporphyrin Stability in Air. The stability of Ru(POR) on pyridine-terminated monolayers in air, in methylene chloride, and in aqueous solutions is surprising, given the relatively rapid oxidation of Ru(POR)(CH₃CN)₂ in polar, noncoordinating solvents. In such cases, the metalloporphyrin absorbs one equivalent of dioxygen, which can be removed under vacuum to recover the initial metalloporphyrin.^{46–48} Ru(POR)(CH₃CN)₂ in toluene or Ru(POR)L₂, where L is pyridine or 1-methylimidazole, in dimethylformamide (DMF) decomposes irreversibly when treated with dioxygen. Dolphin, James,

(44) Everett, W. R.; Fritsch-Faules, I. *Anal. Chim. Acta* **1995**, *307*, 253–268.

(45) Everett, W. R.; Welch, T. L.; Reed, L.; Fritsch-Faules, I. *Anal. Chem.* **1995**, *67*, 292–298.

(46) Farrell, N.; Dolphin, D.; James, B. R. *J. Am. Chem. Soc.* **1978**, *100*, 324–326.

(47) James, B. R.; Addison, A. W.; Cairns, M.; Dolphin, D.; Farrell, N. P.; Paulson, D. R.; Walker, S. *Progress in dioxygen complexes of metalloporphyrins*; Tsutsi, M., Ed.; Plenum: New York, 1979; Vol. 3, p 772.

(48) Smith, P. D.; James, B. R.; Dolphin, D. H. *Coord. Chem. Rev.* **1981**, *39*, 31–75.

(42) Porter, M. D.; Bright, T. B.; Allara, D. L.; Chidsey, C. E. D. *J. Am. Chem. Soc.* **1987**, *109*, 3559–3568.

(43) Duevel, R. V.; Corn, R. M. *Anal. Chem.* **1992**, *64*, 337–342.

and co-workers speculate that the initial oxidation product is an η^2 -bound dioxygen reduced to the level of a peroxide bridging two ruthenium porphyrins. Collman et al. have characterized hydroxy-capped μ -oxo dimers of Ru(IV) as the ultimate oxidation product in the presence of water.^{49,50} In the present case, the initial Ru(II)-dioxygen complex may form reversibly (vide infra), but lack of additional metalloporphyrin, either from diffusion across the surface or from metalloporphyrin in solution, precludes formation of the η^2 -bridged dioxygen intermediate.

Complexes of the type LRu(POR)L', where L is pyridine and L' is a weaker ligand such as acetonitrile, have not been studied, due mainly to difficulties involved in their synthesis: addition of 1 equiv of L to a solution of Ru-(POR)L'₂ produces a mixture of Ru(POR)L₂ and Ru(POR)-L'₂. The inability to add only one strong ligand also means that shish-kebab dimers of the type LRu(POR)L''Ru-(POR)L, where L'' is a bidentate ligand such as pyrazine, are unknown; only higher order, solubility-limited oligomers have been characterized.^{51,52} The ability reported here to conduct a stepwise synthesis of asymmetrically substituted LRu(POR)L'', where L is a monolayer-bound pyridine or imidazole, portends that such dimers and short oligomers may be constructed and studied on the SAM surface. In addition to yielding useful electrochemical information, modular syntheses of surface-confined metalloporphyrin oligomers hold the promise of creating new synthetic templates. The monolayer-coated electrode with its isolated, pendant ligand may be conceptually the largest and most sterically hindered ligand yet designed. It may also be possible to cleave the underlying ester linkage in MUIN-based monolayers⁵⁵ to release shish-kebab dimers and trimers into solution.

Nature of the Distal Ligand. Due to the low absolute surface coverage of metalloporphyrin and the weak spectral signatures of the ligands involved, we are unable to characterize the distal axial ligand present in electrochemical experiments prior to substitution of a known ligand. The porphyrin attachment chemistry utilizes a bis-acetonitrile complex under a dinitrogen ambient. While there is precedent for bis-dinitrogen complexes of naked, four-coordinate Ru(POR),⁵³ the bonding in such complexes is particularly weak, allowing the dinitrogen to be readily removed by evacuation. For all experiments run in the drybox, we believe the distal axial ligand to be acetonitrile. Once samples are removed from the box, it is possible that this ligand is replaced with dioxygen (vide supra), or even water once the sample is subjected to electrochemical analysis.

In one set of experiments, Ru(TTP) attached to a MUIN monolayer was subjected to cyclic voltammetry in methylene chloride within the drybox under a dinitrogen ambient. Formal potentials were measured against an internal standard of acetylferrocene in solution. The same sample was removed from the box, and the cyclic voltammetry was repeated under ambient atmosphere on the benchtop. The formal potential of the Ru(TTP) did not change. While this is not proof that the distal ligand did not change between the two environments, it does show

Table 1. $E_{1/2}$ for Monolayer-Bound and Solution-Phase Ru(POR)^a

proximal ligand	distal ligand	porphyrin	
		OEP	TTP
-MUIN	L ^b	+0.180	+0.406
-MUIN	pyridine	+0.122	+0.346
-MUIN	4,4'-dipyridyl	+0.136	+0.342
-MUIN	pyrazine	+0.185	+0.411
-pyridine	L ^b	+0.044	+0.270
-imidazole	L ^b	-0.139	+0.086
pyridine ^c	pyridine	+0.080 ^d	+0.196
isopropyl	isopropyl	+0.075	+0.308
isonicotinate ^c	isonicotinate		
acetonitrile ^c	acetonitrile	+0.062	+0.234

^a All potentials are reported vs SCE in 0.1 M TBAH/CH₂Cl₂. ^b Originally acetonitrile. ^c Solution-phase measurement. ^d This work and ref 65.

that exchange, if it did take place, proceeded to a product with an identical formal potential. Such a result might be expected for a range of weakly interacting ligands. Whatever the identity of this distal ligand, it can be readily exchanged for pyridine or another nitrogen heterocycle under air: The sample from the benchtop experiment was rinsed and allowed to stand for 30 min in a 10 mM solution of pyrazine in toluene. Subsequent cyclic voltammetry showed that the formal potential had shifted to that observed from identical samples treated with pyrazine solution within the drybox.

Surface Coverage. As illustrated in Figure 2, the limiting surface coverage for Ru(TTP) of 5.7×10^{-11} mol cm⁻² corresponds to an effective area of 290 Å² per porphyrin. This result is in keeping with an idealized commensurate superlattice of porphyrins on the $\sqrt{13} \times \sqrt{13} R30^\circ$ alkanethiolate monolayer. Such a model allows the closest packing of porphyrins with a cross-sectional area of 200 Å², yielding an effective area of 281 Å² per porphyrin.

Even at very dilute surface coverages, we are unable to estimate the total number of ligands on the surface, given the large cross-sectional area of the coordinated metalloporphyrins. Uncomplexed ligands could easily exist within the area shadowed by a complexed porphyrin. In addition, there could be additional, uncomplexed ligands which are free of the porphyrin shadow but are unable to accommodate a porphyrin due to the potential overlap of that porphyrin with a complexed neighbor.

Formal Potentials. Both the nature of the porphyrin ring substituents and the choice of the proximal ligand (that ligand offered by the monolayer for porphyrin axial attachment) can be used to tune the formal potential of surface-complexed metalloporphyrins. As shown in Table 1, TTP shows formal potentials roughly 190 mV more positive than those of the corresponding OEP complex. In moving from 1-alkylimidazole to 4-alkylpyridine to an isonicotinate as the proximal ligand, the formal potential of a coordinated metalloporphyrin can be tuned by roughly 400 mV. When viewed in this fashion, the identity of the distal axial ligand is less significant, offering smaller changes in formal potential on the order of ± 50 mV.

Exchange Rates and Stability of the SAM/Metalloporphyrin Linkage. The stability of Ru(POR) complexes immobilized on monolayers is somewhat surprising in light of ligand exchange studies for similar complexes in solution. The kinetics of ligand exchange for L in Ru-(OEP)(CO)L, where L = 1-methylimidazole, as studied by NMR line shape analysis shows that the first-order exchange of L proceeds with a half-life of 11 s at room

(49) Collman, J. P.; Barnes, C. E.; Swepston, P. N.; Ibers, J. A. *J. Am. Chem. Soc.* **1984**, *105*, 3500-3510.

(50) Collman, J. P.; Barnes, C. E.; Collins, T. J.; Brothers, P. J.; Galaci, J.; Ibers, J. A. *J. Am. Chem. Soc.* **1981**, *103*, 7030-7032.

(51) Collman, J. P.; McDevitt, J. T.; Yee, G. T.; Leidner, C. R.; McCullough, L. G.; Little, W. A.; Torrance, J. B. *Proc. Natl. Acad. Sci. U.S.A.* **1986**, *83*, 4581-4585.

(52) Collman, J. P.; McDevitt, J. T.; Leidner, C. R.; Yee, G. T.; Torrance, J. B.; Little, W. A. *J. Am. Chem. Soc.* **1987**, *109*, 4606-4614.

(53) Camenzind, M. J.; James, B. R.; Dolphin, D. *J. Chem. Soc., Chem. Commun.* **1986**, 1137-1139.

temperature.^{54–56} Furthermore, the kinetics of substitution is generally insensitive to the π -acidity of the ligand trans to the leaving group.⁵⁷ Such exchange is believed to proceed by an S_N1 -type mechanism, where the rate-limiting step is the dissociation of the metal–ligand complex. In the current case of Ru(POR) on MUIN monolayers, the long-term stability as seen in the electrochemical studies argues that if the metal–monolayer dissociation step proceeds at a similar rate on these surfaces, then the monolayer-based ligand recaptures the metalloporphyrin with exceedingly high efficiency. Put differently, even though the surface concentration of ligand on the monolayer is low, the ability of the metalloporphyrin to diffuse away from the ligand before recapture can occur must be exceedingly small. A similar explanation has been advanced recently to explain the persistence of a substitutionally labile, axially ligated cobalt(II) porphyrin on a monolayer-tethered imidazole ligand in aqueous electrolyte.²¹

When another nitrogen-donor ligand, such as pyridine or pyrazine, is present in solution above the monolayer in large concentration, the stability of the SAM–metalloporphyrin linkage is not significantly altered. Qualitative observations indicate that the rate of axial ligand exchange in solution-based Ru(POR)(py)₂ is several orders of magnitude lower than for Ru(POR)(CO)L.⁵⁷ In our SAM-based system, we believe that the distal axial ligand (either acetonitrile or dioxygen, as discussed above) is rapidly exchanged for the heterocyclic nitrogen donor, rendering the resulting heterocyclic nitrogen donor capped, SAM-based metalloporphyrin substitutionally inert.

We hypothesize that the SAM–metalloporphyrin stability before capping with a nitrogen heterocycle is largely due to the hydrophobic nature of the interaction between the bottom of the metalloporphyrin and the shadowed monolayer beneath. While the strength of the van der Waals forces present at this interface is undoubtedly small, the more important feature may be the exclusion of solvent or potential competing ligands from the SAM-based ligand/metalloporphyrin interface. As a general effect, this system argues that while the thermodynamics of complexation between monolayer-based ligands and the metalloporphyrin as described by the equilibrium constant may not be particularly large, steric effects associated with solvent and ligand penetration under the “skirt” of the porphyrin can be dominant in determining the overall stability of such systems.

Aqueous Electroactivity. As shown in Figure 3, sharp cyclic voltammetric features for the aqueous oxidation and reduction of Ru^{II}(POR) are possible when a hydrophobic anion such as hexafluorophosphate is present in the supporting electrolyte. With less hydrophobic anions, the oxidation and reduction of the neutral Ru(POR) is smeared out or rendered indistinct from the background capacitance.

The radically different effects of aqueous and nonaqueous environments on surface-confined Ru(POR) are reversible. Samples may be examined via CV in methylene chloride, yielding results similar to those shown in Figure 1, and then rinsed and placed in aqueous electrolyte. Results similar to those obtained in Figure 3 are obtained. If the sample is then rinsed with water followed by methylene chloride prior to immersion in methylene

chloride with 0.1 M TBAH, results similar to those shown in Figure 1 are obtained again.

The effects of ion pairing between SAM-bound electroactive centers and electrolyte ions, ion penetration into monolayers to reach tethered electroactive centers,⁵⁸ and theoretical interpretations of such behavior^{59–61} have recently been published. In these interpretations, the oxidation of a neutral, SAM-bound complex to a cation in the presence of a pairing anion should shift the peak to more negative potentials as the strength of the ion pairing increases.⁶¹ Alternatively, in the limit where the redox center is embedded within the monolayer, limiting the approach of electrolyte ions to the electroactive center, the voltammetric response broadens and shifts to more positive potentials.⁵⁹

In methylene chloride, a solvent of low dielectric constant, ion pairing should be prevalent. Yet for an oxidized metalloporphyrin/hexafluorophosphate ion pair, with large radii and very low charge densities, the electrostatic interaction driving ion pairing should be minimal compared to that for other possible ion pairs. In an aqueous environment, the large, hydrophobic, pendant metalloporphyrins would be largely unsolvated, creating a region of low permittivity at the outer edge of the SAM which, upon oxidation, would be populated only by relatively hydrophobic anions which would not be able to approach the plane of the metalloporphyrins without shedding their solvation spheres. This situation would correspond to the second limit outlined above. In the absence of hexafluorophosphate, the broadened cyclic voltammetric response would argue that charge neutralization of the cationic metalloporphyrins by the supporting electrolyte anion is incomplete, resulting in only a small potential drop across the plane of the remaining unoxidized metalloporphyrins. Only upon addition of the hexafluorophosphate anion does a significant portion of the potential drop across the electroactive centers. We speculate that the special status of the hexafluorophosphate anion in evincing near-ideal electrochemistry in an aqueous electrolyte is due to a favorable Gibbs energy of transfer for hexafluorophosphate between the aqueous electrolyte and the region about and under the tethered porphyrin.^{62,63} Given the linkage between the porphyrin and the top of the underlying decanethiol monolayer, it is possible that the porphyrin tilts upon oxidation of the ruthenium center due to the resulting intercalation of the desolvated hexafluorophosphate anion.

Acid/Base Chemistry. At first glance, there would appear to be a strong driving force for proton transfer from the unreacted carboxylic acid groups present in the MUA monolayer and the pyridines attached via the amide linkage in monolayers produced via Scheme 1B. The pK_a of the carboxylic acid in monolayers of MUA is 5.5,⁶⁴ while that of 4-(aminomethyl)pyridine is 8.5. By forming the amide linkage in buffered solution and then rinsing with ethanol prior to metalloporphyrin attachment in toluene, one can present a deprotonated pyridine for axial attachment.

(58) Rowe, G. K.; Creager, S. E. *Langmuir* **1991**, *7*, 2307–2312.

(59) Smith, C. P.; White, H. S. *Anal. Chem.* **1992**, *64*, 2398.

(60) Smith, C. P.; White, H. S. *Langmuir* **1993**, *9*, 1.

(61) Andreu, R.; Calvente, J. J.; Fawcett, W. R.; Molerio, M. *J. Phys. Chem. B* **1997**, *101*, 2884–2894.

(62) Schroeder, U.; Wadhawan, J.; Evans, R. G.; Compton, R. G.; Wood, B.; Walton, D. J.; France, R. R.; Marken, F.; Page, P. C. B.; Hayman, C. M. *J. Phys. Chem. B* **2002**, *106*, 8697–8704.

(63) Kondo, T.; Okamura, M.; Uosaki, K. *J. Organomet. Chem.* **2001**, *637–639*, 841–844.

(64) Creager, S. E.; Clarke, J. *Langmuir* **1994**, *10*, 3675–3683.

(65) Brown, G. M.; Hopf, F. R.; Meyer, T. J.; Whitten, D. G. *J. Am. Chem. Soc.* **1975**, *97*, 5385–5390.

(54) Eaton, S. S.; Eaton, G. R.; Holm, R. H. *J. Organomet. Chem.* **1971**, *32*, C52–C54.

(55) Eaton, S. S.; Eaton, G. R.; Holm, R. H. *J. Organomet. Chem.* **1972**, *39*, 179–195.

(56) Eaton, S. S.; Eaton, G. R. *Inorg. Chem.* **1977**, *16*, 72–74.

(57) Holloway, C. E.; Stynes, D. V.; Vuik, C. P. J. *J. Chem. Soc., Dalton Trans.* **1982**, *1*, 95–101.

Conclusions

We have demonstrated two approaches to the modular assembly of metalloporphyrin-decorated alkanethiolate monolayers on gold. In the first approach, deposition of the underlying monolayer from a two-component solution composed of ligand-terminated and diluent alkanethiols provides considerable control over the number of ligand sites presented for subsequent metalloporphyrin attachment. In the second approach, attachment of the ligand after monolayer assembly, followed by subsequent metalloporphyrin attachment, allows a wide range of monolayer thicknesses and ligands to be explored quickly with commercially available components.

The use of isonicotinate derivatives as the ligand for metalloporphyrin attachment leads to monolayer-bound electroactive centers exhibiting sharp, air-stable electrochemistry in methylene chloride. Aqueous electrochemistry is possible using hexafluorophosphate in the supporting electrolyte.

The distal axial ligand in such systems can be readily exchanged in order to tune the formal potential of the

system or to allow for subsequent complexation of additional metalloporphyrins through bidentate ligands. This modular approach may be useful in the monolayer-supported synthesis of shish-kebab oligomers, especially those which are asymmetrically substituted.

Efforts are ongoing to build extended supramolecular structures, to explore the multivalent characteristics of metalloporphyrin oligomers created this fashion, to characterize the kinetics of axial ligand substitution in monolayer-based metalloporphyrins, and to utilize the expected low solvent reorganization energy of metalloporphyrins in aqueous electrolytes to study the dependence of electron-transfer kinetics with distance.

Acknowledgment. The authors acknowledge many helpful discussions with Dr. Sandra B. Sachs. This work was supported by National Science Foundation Grant CHE-9612725.

LA026948J